Asian Journal of Chemistry; Vol. 38, No. 2 (2026), 443-451
ASIAN JOURNAL OF CHEMISTRY
https://doi.org/10.14233/ajchem.2026.35064

Therapeutic Potential of Disubstituted [{[5-(2-Chloro phenyl)-1,3,4-thiadiazole-2-yl]imino}-methyl]phenyl Derivatives as α-Amylase Antagonists: Synthesis, *In silico* and *In vitro* Screening

D. RAVI SANKARA REDDY*, and T. SRINIVASARAO

Department of Pharmaceutical Chemistry, University College of Pharmaceutical Sciences, Acharya Nagarjuna University, Nagarjuna Nagar-522510, India

*Corresponding author: E-mail: drsrpharma@gmail.com

Received: 14 October 2025 *Accepted*: 9 January 2026 *Published online*: 31 January 2026 AJC-22262

During the last few decades medicinal chemist focus turns to the novel heterocyclic moiety thiadiazole having similar stereotype with thiazole ring with hypoglycemic activity. Henceforth, this study aims to synthesise the designed novel 2,5-diarylsubstituted 1,3,4 thiadiazole derivatives (TDZ) by two step process using microwave irradiation method. The title compounds with electron withdrawing groups (nitro), electron donating groups (hydroxy, dimethyl amine) were synthesized from condensation of thiosemicarbazide with *o*-chlorobenzoic acid in presence of acidic catalyst followed by the condensation of the intermediate with substituted benzaldehydes under microwave irradiation. Molecular docking studies against α-amylase using Autodock and Schrödinger, molecular dynamic simulation studies using Growmacs and *in vitro* antidiabetic activity by α-amylase inhibition assay was performed to all the 2,5-diarylsubstituted 1,3,4-thiadiazole derivatives. There is a correlation of *in silico* and *in vitro* results, derivatives **TDZ7** and **TDZ2** (61% and 59%) showed significant α-amylase inhibition than the miglitol (81%) at 1000 µg/mL concentration. Molecular modelling studies demonstrates that derivatives **TDZ2** and **TDZ7** against 7taa (-8.67 and -7.82 kcal/mol), 1b2y (-4.8 and -4.5 kcal/mol), respectively, possess least binding energies than that of the standard drugs miglitol (-5.05 kcal/mol) and metformin (-8.19 kcal/mol) against 7taa with enzyme inhibition constant 442.33 nM, 1.85, 197.74 µM and 998 nM, respectively. All the ligands and standard drugs showed hydrophilic interactions with active site amino acids, with varying distances. Further research is needed to get the active derivatives with hypoglycemic potential.

Keywords: 2,5-Diarylsubstituted 1,3,4-thiadiazole, α-Amylase, Molecular docking, Dynamic simulation, Hypoglycemic activity.

INTRODUCTION

Heterocyclic compounds with thiadiazole ring exhibit unique chemical properties due to the presence of sulphur and nitrogen atoms. It is a planar, five-membered heterocyclic ring with a high degree of aromaticity and making it relatively stable [1]. The sulphur atom imparts a degree of electrophilicity, while the nitrogen atoms contribute to the ring's basicity. These properties enable thiadiazole derivatives to participate in various chemical reactions, such as nucleophilic substitution and electrophilic addition, making them valuable intermediates in organic synthesis [2,3]. One of the isomers 1,3,4-thiadiazole (TDZ) with aryl substitution at 2nd and 5th positions having promising biological properties like antimicrobial [2-5], anti-oxidant [4,6], anti-inflammatory [6], anticancer [5,7], analgesic activities [8], antidiabetic activity [9], *etc*.

According to WHO, diabetes mellitus (DM) is a chronic disorder caused due to the body's inability to secrete or properly utilize insulin [10], leading to high blood sugar levels. This can result from autoimmune destruction of insulin-producing cells (Type 1), insulin resistance and impaired insulin secretion (Type 2) or other factors such as genetics, obesity and physical inactivity. Improper carbohydrate metabolism can be a significant risk factor [11]. Managing carbohydrate intake is crucial with diabetes to regulate blood glucose levels. α-Amylase is one such metabolizing enzyme and plays a vital role in diabetes by breaking down starch into simple sugars, which are then absorbed into the bloodstream, causing rise in blood glucose levels [12,13]. α-Amylase inhibitors have also been explored as a potential therapeutic approach to manage postprandial blood glucose spikes in diabetes [13]. Hence, this study was targeted to design, synthesis and evaluate the 2,5-

diarylsubstituted 1,3,4-thiadiazole derivatives potential towards the α-amylase enzyme ultimately in diabetes treatment.

In this work, we design and synthesise novel 2,5-diaryl-substituted 1,3,4-thiadiazole derivatives by two step process using microwave irradiation method as potential α-amylase inhibitors for antidiabetic therapy. By modulating electronic substituents on the thiadiazole scaffold, the structure-activity relationships were also explored and an integrated *in silico-in vitro* medicinal chemistry strategy was employed to identify promising lead compounds for further hypoglycemic drug development.

EXPERIMENTAL

All the chemicals and solvents purchased from various commercial sources like Qualigens, S.D. Fine Chem and E. Merck for the synthesis and biological screening. Pre-coated aluminum silica gel plates used for TLC. Gallenkamp MFB 595 010M melting point apparatus used for determining the uncorrected melting point in open capillary tube. The Bruker Bioscience, Digital FT-NMR spectrometer used to record the NMR spectra (both ^{1}H and ^{13}C) in DMSO-d_6 at 300 MHz. Using FTIR-8400 spectrometer, title compounds infrared spectra were captured by KBr pellet method. The M+1 peak analysed by Shimadzu LC/MS IT-TOF system (Shimadzu, Tokyo, Japan).

General procedure for synthesis of 2,5-diaryl-1,3,4-thiadizoles (TDZ1-TDZ9): Initially, the intermediate was synthesised from *o*-chlorobenzoic acid (0.1 mol) and thiosemicarbazide (0.1 mol) in presence of 10 mL of methanol and conc. H_2SO_4 at 300 Watts microwave irradiation for 4 min. Then, the equimolar concentration of intermediate 2-amino-5-(2-chlorophenyl)-1,3,4-thiadiazole (0.05 mol) and substituted benzaldehydes dissolved in 6 mL of methanol were mixed followed by the addition of six drops of glacial acetic acid and then irradiated in microwave with power level 3 (300 W) for 4-5 min to obtain title compounds **TDZ1-TDZ9** (**Scheme-I**). The white colour product obtained after addition of crushed ice, gets filtered, washed and recrystallised with absolute alcohol [14].

3-[{[5-(2-Chlorophenyl)-1,3,4-thiadiazol-2-yl]imino}-methyl]phenol (TDZ1): Yield: 60%, m.p.: 200-202 ºC; IR (KBr, ν_{max}, cm^{-1}): 3132 (Ar–C–H), 2894 (N=C–H), 1683 (C=C), 1509 (C=N), 1230 (Ar–C–O), 825 (C–Cl), 743 (C–S–C); ^{1}H NMR (DMSO-d_6, δ ppm): 11.25 (s, =C–H), 9.80 (s, Ar-OH), 8.06-6.70 (m, Ar-8H); ^{13}C NMR (400 MHz, DMSO-d_6, δ ppm): 111.5-159.7 (12 Ar–C), 163.7-191.4 (3C, imine). Mass (*m/z*): $[M+H]^+$ calcd.: $C_{15}H_{10}ClN_3OS$, 315.01; found: 316.01.

***N*-[5-(2-Chlorophenyl)-1,3,4-thiadiazol-2-yl]-1-(4-nitrophenyl)methanimine (TDZ2):** Yield: 86%, m.p.: 210-211 ºC; IR (KBr, ν_{max}, cm^{-1}): 3020 (Ar C–H), 2964 (N=C–H), 1669 (C=N), 1536 (C=C), 1512 (Ar N=O), 843 (C–Cl), 723 (C–S–C); ^{1}H NMR (DMSO-d_6, δ ppm): 11.4 (s, 1H, imine), 8.97-8.05 (m, 8H, aromatic); ^{13}C NMR (400 MHz, DMSO-d_6, δ ppm): 128.7-149.05 (12C aromatic), 160.7-181.7 (3C, imine). Mass (*m/z*): $[M+2]^+$ calcd.: $C_{15}H_9ClN_4O_2S$, 344.01; found: 346.2.

***N*-[5-(2-Chlorophenyl)-1,3,4-thiadiazol-2-yl]-1-(4-methoxyphenyl)methanimine (TDZ3):** Yield: 73%, m.p.: 185-187 ºC. IR (KBr, ν_{max}, cm^{-1}): 3042 (Ar C–H), 2935 (N=C–H), 1652 (C=N), 1514 (C=C), 1236 (Ar C–O), 824 (C–Cl), 757 (C–S–C); ^{1}H NMR (DMSO-d_6, δ ppm): 11.32 (s, 1H, imine), 8.16-6.9 (m, 8H, aromatic), 3.78 (3H, methyl). ^{13}C NMR (400 MHz, DMSO-d_6, δ ppm): 117.5-139.7 (12 Ar–C), 161.7-191.7 (3C, imine), 58.5 (1C, methoxy). Mass (*m/z*): $[M+H]^+$ calcd.: $C_{16}H_{12}ClN_3OS$, 329.01; found: 331.01.

4-[{[5-(2-Chlorophenyl)-1,3,4-thiadiazol-2-yl]imino}-methyl]phenol (TDZ4): Yield: 83%, m.p.: 215-217 ºC; IR (KBr, ν_{max}, cm^{-1}): 3042 (ArC–H), 2935 (N=C–H), 1687 (C=N), 1522 (C=C), 1277 (Ar–C–O), 822 (C–Cl), 723 (C–S–C); ^{1}H NMR (DMSO-d_6, δ ppm): 11.25 (s, 1H, imine), 8.5 (s, 1H, phenol), 8.06-6.7 (m, 8H, aromatic); ^{13}C NMR (400 MHz, DMSO-d_6, δ ppm): 101.5-159.7 (12C, aromatic), 158.7-189.4 (3C, imine), Mass (*m/z*): $[M+H]^+$calcd.: $C_{15}H_{10}ClN_3OS$: 315.01; found: 314.60.

***N*-[5-(2-Chlorophenyl)-1,3,4-thiadiazol-2-yl]-1-(3-nitrophenyl)methanimine (TDZ5):** Yield: 74%, m.p.: 205-207 ºC; IR (KBr, ν_{max}, cm^{-1}): 3025 (Ar C–H), 2892 (N=C–H), 1704 (C=N), 1599 (C=C), 1514 (Ar-N=O), 843 (C–Cl), 738 (C–S–C). ^{1}H NMR (DMSO-d_6, δ ppm): 11.11 (s, 1H, imine), 8.51-7.12 (m, 8H); ^{13}C NMR (400 MHz, DMSO-d_6, δ ppm): 117.5-139.7 (12 Ar–C), 159.7-187.7 (3C, imine). Mass (*m/z*): $[M+H]^+$ calcd.: $C_{15}H_9ClN_4O_2S$: 344.29; found: 343.10.

1-(2-Chlorophenyl)-N-[5-(2-chlorophenyl)-1,3,4-thiadiazol-2-l]methanimine (TDZ6): Yield: 78%, m.p.: 145-147 ºC; IR (KBr, ν_{max}, cm^{-1}): 3159 (Ar C–H), 2896 (N=C–H), 1685 (C=N), 1473 (C=C), 812 (C–Cl), 755 (C–S–C); ^{1}H NMR (DMSO-d_6, δ ppm): 11.8 (s, HC=N), 8.40-7.95 (m, 8H, arom.); ^{13}C NMR (400 MHz, DMSO-d_6, δ ppm): 124.7-147.5 (12C, aromatic), 160.7-191.7 (3C, imine). Mass (*m/z*): $[M+H]^+$ calcd.: $C_{15}H_9Cl_2N_3S$: 334.01; found: 335.2.

1-(2-Chlorophenyl)-N-[5-(4-nitrophenyl)-1,3,4-thiadiazol-2-yl]methanimine (TDZ7): Yield: 73%, m.p.: 210-212 ºC; IR (KBr, ν_{max}, cm^{-1}): 3093 (Ar C–H), 2892 (N=C–H), 1579 (C=N), 1514 (C=C), 1516 (Ar N=O), 814 (C–Cl), 746 (C–S–C); ^{1}H NMR (DMSO-d_6, δ ppm): 8.40-8.05 (m, 8H, arom.), 11.7

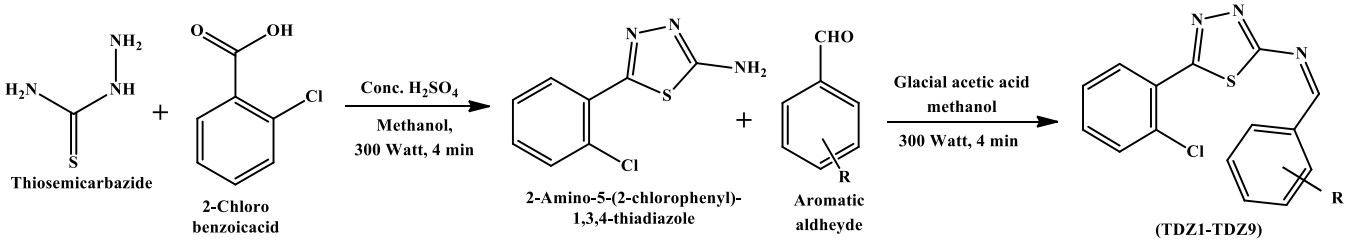

Scheme-I: Synthetic scheme of title compounds (**TDZ1-TDZ9**)

(s, 1H, imine); ^{13}C NMR (400 MHz, DMSO-d_6, δ ppm): 124.7-147.5 (12 Ar–C), 160.7-191.7 (3C, imine). Mass (*m/z*): $[M+H]^+$ calcd.: $C_{15}H_9ClN_4O_2S$: 344.01; found: 345.21.

4-[{[5-(2-Chlorophenyl)-1,3,4-thiadiazol-2-yl]imino}-methyl]-*N*,*N*-dimethylaniline (TDZ8): Yield: 75%, m.p.: 110-111 ºC; IR (KBr, ν_{max}, cm^{-1}): 3153 (Ar C–H), 2898 (N=C–H), 1655 (C=N), 1487 (C=C), 812 (C–Cl), 724 (C–S–C); ^{1}H NMR (DMSO-d_6, δ ppm): 11.32 (s, 1H, imine), 8.16-6.9 (m, 8H, aromatic), 3.81 (s, 6H, methyl); ^{13}C NMR (400 MHz, DMSO-d_6, δ ppm): 115.5-137.7 (12C, aromatic), 161.7-191.7 (3C, imine), 60.5 (2C, methyl); Mass (*m/z*): $[M+H]^+$ calcd.: $C_{17}H_{15}ClN_4S$: 342.01; found: 344.98.

2-[{[5-(2-Chlorophenyl)-1,3,4-thiadiazol-2-yl]imino}-methyl]phenol (TDZ9): Yield: 65%, m.p.: 180-182 ºC; IR (KBr, ν_{max}, cm^{-1}): 3046 (Ar C–H), 2827 (N=C–H), 1597 (C=N), 1594 (C=C), 1270 (Ar–C–O), 823 (C–Cl), 747 (C–S–C); ^{1}H NMR (DMSO-d_6, δ ppm): 11.25 (s, 1H, imine), 9.8 (s, 1H, phenol), 8.06-6.7 (m, 8 Ar-H); ^{13}C NMR (400 MHz, DMSO-d_6, δ ppm): 101.5-149.7 (12 Ar–C), 161.7-187.4 (3C, imine). Mass (*m/z*): $[M+H]^+$ calcd.: $C_{15}H_{10}ClN_3OS$: 315.01; found: 317.58 [M+2].

Molecular docking: Molecular docking (MD) is one of the molecular modelling techniques performed by using computer in which the best fit stable orientation of ligand macromolecule complex with least binding energy was predicted. It was performed using AUTODOCK [15,16] involves number of steps. All the ligand structures were drawn using the software Chem Draw Ultra 12.0, energy minimised by using chem 3D pro of Chem Bio Office Suite. A amylase (pdb id: 7taa) X-ray crystal structure complexed with acarbose [17,18] having resolution (1.98 Å) was selected from protein data bank. All the heteroatoms and co-crystal ligands were removed from 7taa using discovery studio. The target proteins were prepared for docking by generating grid box with spacing 0.349 Å, the grid parameter files and convert to log files. Docking performed for 10 runs with 100 cycles generates the dock parameter files and convert to dock log files using command prompt. Finally, the interactions of best fit ligand complex using discovery studio visualize were analysed [16].

Molecular docking using Schrödinger

Protein preparation: The structure of human pancreatic α-amylase in complex with acarbose (PDB ID: 1B2Y) downloaded from the RCSB protein data bank database [19] has no mutations and the resolution of 3.20 Å. The proteins were prepared prior to perform docking using the 'protein preparation wizard' from Schrödinger Maestro to fix all problems as the originally downloaded PDB files do not have proper bonding configuration, neither the hydrogen atoms are satisfied to further use for any studies. The protein preparation workflow starts with assigning bond orders by using CCD database and corresponding hydrogen atoms were added to optimize the process. The heterostates were generated using Epik at a pH range of 7.0 ± 2.0. Zero bond orders were assigned to metal centers and disulfide bonds, and all crystallographic water molecules located beyond 5.0 Å from the active site were removed. Further, we have assigned the H-bonds to fix all the problems in protein and minimised them with the OPLS3e forcefield after removing the water molecules with less than 3.0 Å of heteroatoms [20].

Ligand preparation: The structures of 2,5-disubstituted 1,3,4-thiadiazole derivatives (**TDZ1-TDZ9**) were drawn using ChemDraw 12.0 software and generate the smiles notation. Further, the 'Lig Prep wizard' was used to prepare the ligands. All TDZ molecules were initially constructed in 2D format and were therefore unsuitable for docking. Consequently, the structures were converted to 3D conformations and energy-minimized using the OPLS3e force field prior to docking studies. Then, the Epik module was employed to generate the most probable ionization and tautomeric states of the ligands at a physiological pH of 7.0 ± 2.0.

Active site calculation and grid box generation: The active site of the protein pancreatic α-amylase (1B2Y) was computed using the 'Site Map' module in the Schrödinger suite. The active site was calculated by cropping site maps at 4 Å from the closest site point, which produced a total of four active sites and identifying the top-ranked possible receptor binding sites. The 'receptor grid generation' wizard generated the grid file on the active site at which modified acarbose binds. The grid was calculated around site1 and the box size was expanded to fit the entire active site at which molecular docking was then carried out.

MMGBSA calculation: Molecular mechanics energies combined with generalised born and surface area continuum solvation (MM-GBSA) methods are popular approaches to estimating the free energy of the binding of small ligands to biological macromolecules. the Prime MMGBSA in maestro was used for evaluating the docked pose of the 9 title compounds from extra precision (XP). These poses were taken as inputs for the energy minimisation of the protein-ligand complexes, the free protein and the free ligands. The potential energy of each frame was decomposed into individual energy contributions such as hydrogen bond, van der Waals, electrostatic and solvation energies. The binding free energy was calculated as the sum of these energy terms [21]. The docking methodology was confirmed by calculating the root mean square deviation (RMSD) of docking the native ligand (co-crystal ligand, acarbose) with the receptor [22].

Molecular dynamic simulation studies: After analyzing the protein-ligand interactions, top three complex (docking score) from docking was taken for the MD simulation studies. Growmacs was used to run the MD simulation to elucidate the stability of the 2,5-disubstituted 1,3,4-thiadiazole derivatives. Input files were created with CHARMM GUI server solution builder. The SPC water model ran for 100ns for dynamic studies. Ion and salt placement within 20 Å were excluded from making the simulation neutralised. Further, using the Charmm 27 forcefield, the complex minimised its energies by heating and equilibrium processes before the production run of MD simulations [23,24]. The steepest descent minimisation protocol was used against the complexes at 0-300 K. Further, with the time step of 100 ps, the system normalised in an equilibrium state at 1000 frames. The final production run was kept for 100 ns and 1.01325 atm pressure for complexes applying the NPT ensemble. RMSD, RMSF and bond analysis were performed with gmx scripts from trajec-

tory. The MD graphics were created with Qt Grace tool and animation videos with pymol.

***In vitro* antidiabetic activity:** To determine α-amylase inhibition, the α-amylase inhibition assay was carried out with minor modifications in accordance with the Rafaqat Hussain technique [25-28]. The standard medication miglitol was made along with an equal volume (0.5 mL) of α-amylase (0.5 mg/mL) in phosphate buffer and derivatives **TDZ1-TDZ9** and standard drug (100 and 500 μg/mL). Both solutions were incubated at 25 ºC for 10 min. Subsequently, 0.5 mL of 1% (w/v) starch solution and 0.02 M phosphate buffer were added, and the reaction mixture was further incubated for 10 min. The reaction was then terminated by the addition of dinitrosalicylic acid (DNSA), and the resulting colour development was monitored to assess enzymatic activity. Then cool the mixture and diluted with distilled water after being incubated in boiling water for 5 min. The following formulas were used to determine the percentage inhibition from the reported absorbance values.

$$\text{Inhibition (\%)} = \frac{A_{control} - A_{sample}}{A_{control}} \times 100$$

***In vitro* antioxidant activity:** To determine the radical scavenging potential (antioxidant) of all 9 novel compounds using hydrogen peroxide (H_2O_2) scavenging assay which is carried out by following previous literature [29-31]. Different concentrations (100, 150 and 200 μg/mL) of sample **TDZ1** to **TDZ9** and standard drug was prepared and incubated with the H_2O_2 buffer solution for 10 min separately. A control solution was prepared with DMSO in phosphate buffer saline. Absorbance was measured at 230 nm wavelength using UV-visible spectrophotometer. Ascorbic acid (AA) was taken as a standard to compare antioxidant potential of **TDZ1-TDZ9**. And the percentage of hydrogen peroxide scavenging was calculated using the following formula.

$$\text{Inhibition (\%)} = \frac{A_{control} - A_{sample}}{A_{control}} \times 100$$

RESULTS AND DISCUSSION

The synthesised novel 2,5-diaryl substituted-1,3,4-thiadiazole (**TDZ1-TDZ9**) compounds were carefully examined by TLC throughout the reaction and the product yields with 65-86%. The functional groups present in the title compounds (**TDZ1-TDZ9**) include aromatic CH stretching from 3159-3020 cm^{-1} is due to the sp^2 hybridised carbon-carbon (C=C) and the imine (C=N) stretching vibrations were observed in the regions 1599-1473 cm^{-1} and 1704-1579 cm^{-1}, which fall within the characteristic ranges typically assigned to C=C stretching (1600-1400 cm^{-1}) and C=N stretching (1690-1690 cm^{-1}), respectively. In addition, the imine C–H stretching vibrations appeared in the range 2964-2827 cm^{-1}, consistent with the expected C–H stretching region of 2900-2800 cm^{-1}. Moreover, the deviation in the spectral values from the normal ranges is due to the presence of electron donating and withdrawing group environment of the derivatives. ^1H and ^{13}C NMR spectral values of all the derivatives are within the normal range.

Molecular docking: The docking results revealed that all **TDZ1-TDZ9** ligands against α-amylase 7TAA exhibited good binding affinity ranging from -6.87 to -7.82 kcal/mol and the standard drugs miglitol (-5.05) and metformin (-8.19) presented in Table-1. Ligands **TDZ1-TDZ9** having enzyme inhibition constant values about 442.33 nM to 9.27 μM and the standard drugs is about 197.74 μM and 998 nM, respectively. The enzyme inhibition is particularly due to the molecular interactions of ligands at the active site of α-amylase enzyme shown in Fig. 1. The key interactions of top ligand **TDZ2** found that 4 hydrogen bonds with amino acid ARG A 344, GLN A 35, HIS A 80 and TYR A 79, 1 carbon hydrogen bond with amino acid ASP A 340, 1 pi-sigma bond with TYR A 82, 1 pi-sulphur bond with HIS A 80, 2 pi-pi stacking with TYR A 82 and HIS A 80, 2 pi-pi T-shaped bond with TYR A 82 and TRP A 83, 9 van der Waal interactions. Like this, **TDZ7** forms 2 hydrogen bonds with amino acid HIS A 210 and ARG A 344, 4 ionic interactions with amino acid ASP A 206, ASP A 297, ASP A 340 and HIS A 80, 1 pi-pi stacking with amino acid HIS A 80, 2 pi-alkyl bonds with amino acid TRP A 83 and HIS A 80. Ligand **TDZ5** forms 3 conventional hydrogen bonds with amino acid ARG A 344 and TYR A 79, 4 ionic bonds with ASP A 206, ASP A 297, HIS A 80 and ASP A 340, 1 pi-pi stacking with TYR A 82, 1 pi-pi T-shaped bond with amino acid TRP A 83, 2 pi-alkyl interactions with amino acid HIS A 122 and TYR A 82 as seen in Fig. 1. There are 4 common interacting amino acids (ASP A 340, HIS A 80, TRP A 83, ARG A 344) in all the ligands with different type of bonds like hydrogen bond, ionic bond, pi-pi stacking, van der Waal interactions as depicted in Figs. 1 and 2. The molecular interactions of standard drug metformin are 3 hydrogen bonds with ASP A 297, 5 van der Waal bonds with HIS A 100, THR A 207, ARG A 204, HIS A 296, ARG A 344, salt bridge and attractive charges with amino acid TRP A 206, GLU A 230, ASP A 297, 1 pi-sigma bond with TYR A 82 whereas miglitol forms 7 van der Waal interactions with HIS A 296, TYR A 82, HIS A 122, THR A 207, LEU A 166, 232, ASP A 297, 6 hydrogen bonds with ASP A 206, ARG A 204 and GLU A 2320, 1 carbon-hydrogen bond with amino acid ASP A 206 as seen in Fig. 1.

The glide scores of the ligand protein complexes indicates the binding affinity of the designed ligands against α-amylase (pdb id: 1B2Y) active pocket range from -4.515 to -4.822 kcal/mol (Table-2). Molecular interactions were studied using pymol, mostly all the derivatives have common hydrogen bonds with aminoacid GLN 63 (between amine hydrogens and N4 nitrogen of thiadiazole moiety), hydrophobic interaction with TRP 58 (between indole ring and benzyl) and TYR 62 (between phenyl and *o*-chlorophenyl ring). Apart from these, ligands **TDZ1**, **TDZ3**, **TDZ4**, **TDZ5**, **TDZ6** and **TDZ7** displayed another hydrogen bond with amino acid GLN 63 between amine hydrogen and ligand imine nitrogen, but **TDZ2** having hydrophobic pi-lone pair bond with amino acid TRP 58 between indole ring and NO_2 group (Fig. 3). Even though ligand forms same type of bonds with binding pocket amino acids, their energy differences is due to the varying bond distance. And ligand **TDZ2** having least docking score is due to the presence of extra hydrophobic bond which gives strong affinity. According to MM-GBSA, a binding free energy

TABLE-1
DOCKING SCORES, HYDROGEN BOND INTERACTING RESIDUES WITH DISTANCES OF **TDZ1-TDZ9** AGAINST 7taa

Code	Binding energy (kcal/mol)	Inhibition constant	Conventional hydrogen bonds		Interacting atoms	
			No.	Amino acid (distance Å)	Protein	Ligand
TDZ1	-7.24	4.91 µM	2	ASP 206(2.08)	O (carboxy)	H (Hydroxy)
				ARG 344 (2.14)	H (amine)	N (thiadiazole)
TDZ2	-8.67	442.33nM	4	GLN 35 (1.78)	H (amine)	O (nitro)
				TYR 79 (2.17)	H (hydroxy)	O (nitro)
				HIS 80 (2.90)	H (imidazole)	O (nitro)
				ARG 344 (1.94)	H (amine)	N (Thiadiazole)
TDZ3	-6.87	9.27 µM	1	ARG 344 (2.14)	H (amine)	N (Thiadiazole)
TDZ4	-7.33	4.5 µM	2	TYR 79 (2.20)	H (hydroxy)	O (hydroxy)
				ASP 340 (1.75)	O (carboxy)	H (hydroxy)
TDZ5	-7.73	2.15 µM	2	ARG 344 (1.89, 2.60)	H (amine), H (amine)	N (Thiadiazole), N (imine)
TDZ6	-7.55	2.94 µM	1	ARG 344 (1.94)	H (amine)	N (Thiadiazole)
TDZ7	-7.82	1.85 µM	2	HIS 210 (2.52)	H (imidazole)	O (nitro)
				ARG 344 (1.94)	H (amine)	N (Thiadiazole)
TDZ8	-6.97	7.73 µM	1	ARG 344 (1.94)	H (amine)	N (Thiadiazole)
TDZ9	-6.91	8.59 µM	3	ARG 204 (2.22)	H (amine)	O (hydroxy)
				HIS 296 (3.0)	H (amine)	O (hydroxy)
				ASP 297 (1.92)	O (carboxy)	H (hydroxy)
Std1	-5.05	197.74 µM	6	ARG 204 (1.72)	H (amine)	O (hydroxy)
				ASP 230 (1.92, 1.78)	O (carboxy)	H (hydroxy)
				GLU 230 (2.07, 2.36, 2.90)	O (carboxy)	H (hydroxy)
Std2	-8.19	998 nm	3	ASP 297 (1.94, 2.04, 2.16)	O (carboxy)	H (amine)

Std1. Miglitol, Std2. metformin

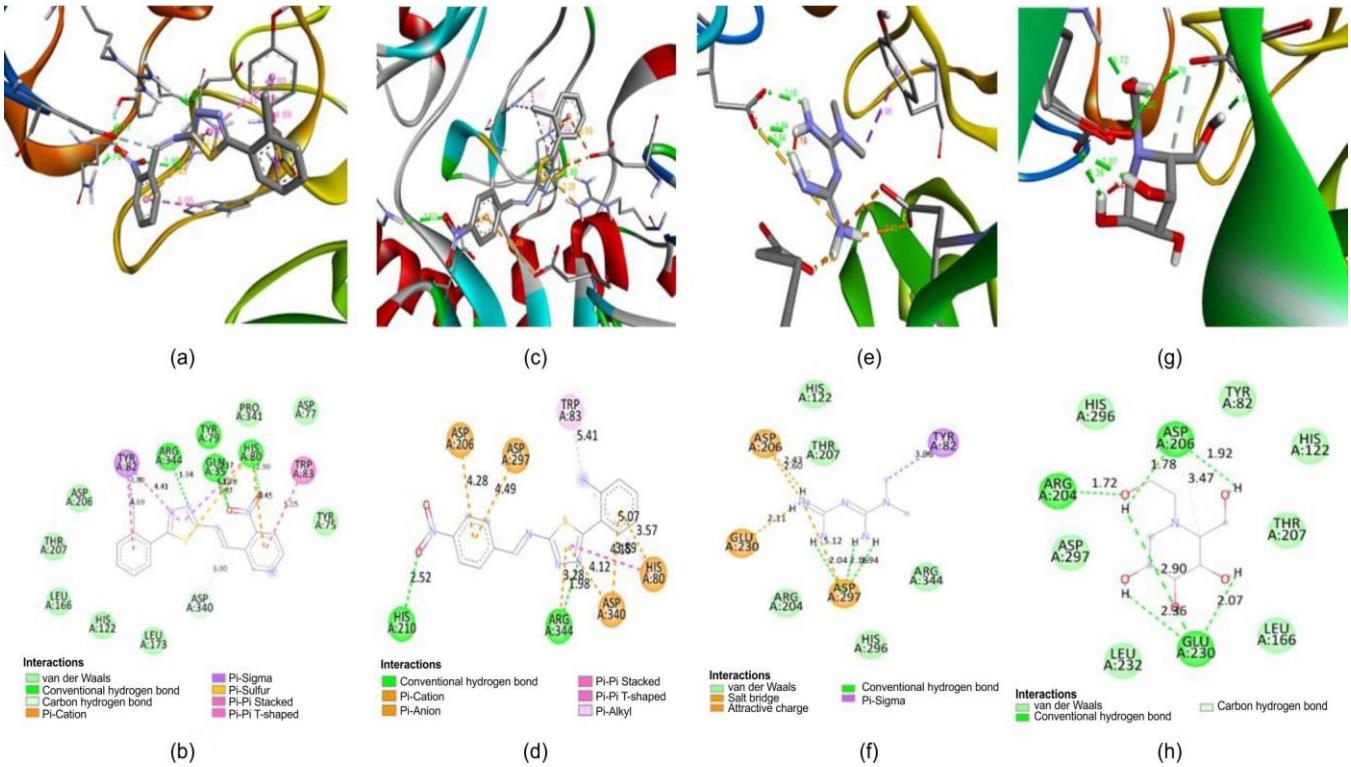

Fig. 1. Atomic interactions of top ligands and standard drugs against α-amylase; (a, b) 3d, 2d view of **TDZ2**; (c, d) 3d, 2d view of **TDZ7**; (e, f) 3d, 2d view of metformin; (g, h) 3d, 2d view of miglitol

analysis was carried out for the nine protein-ligand complexes to assess the ligand affinity to the target protein. MM-GBSA binding free energy is more efficient than glide score [32] (Table-2). The values ranging from -30.62 to -37.92 kcal/mol indicates strong binding affinity and stable complexes.

Molecular dynamics simulation analysis: To assess the stability of protein-ligand complexes that are generated by the putative antidiabetic agents **TDZ2**, **TDZ3** and **TDZ7** with α-amylase. Based on the MMGBSA results, top ligands **TDZ2**, **TDZ3** and **TDZ7** with least binding free energy were selected

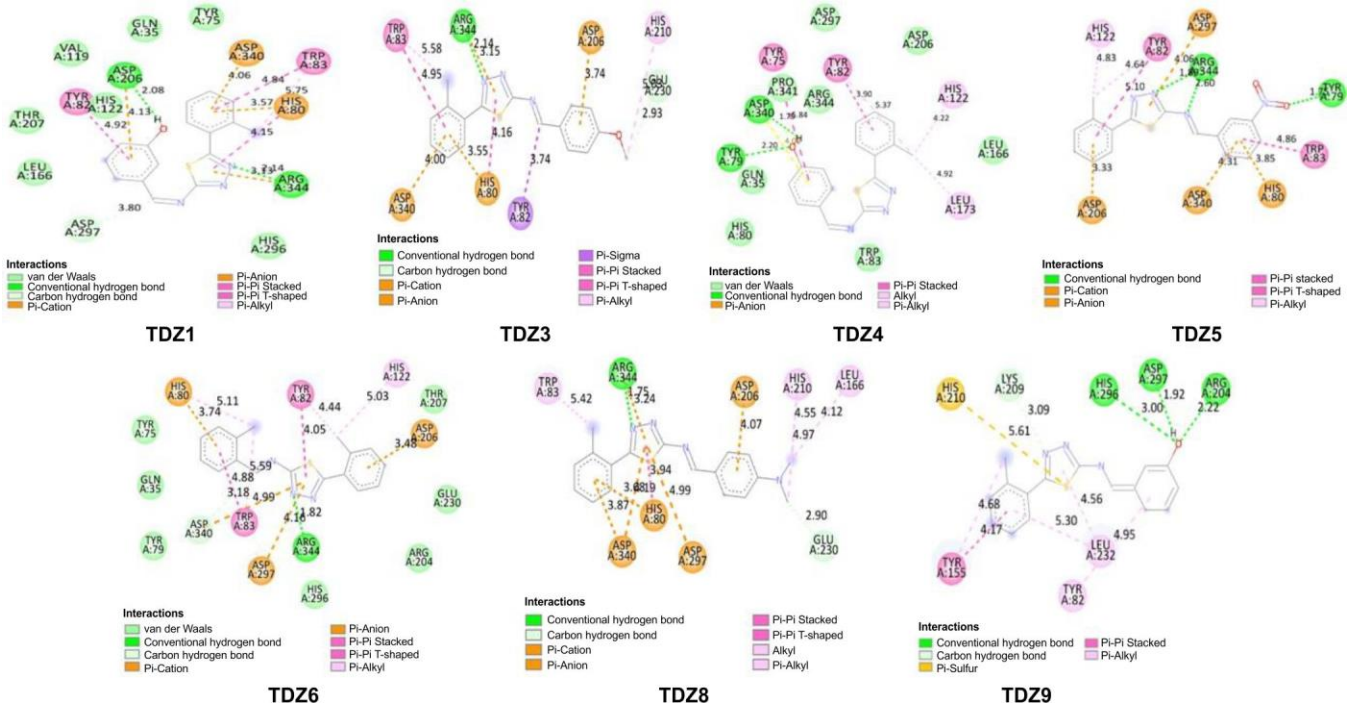

Fig. 2. The 2d view of interactions of ligand enzyme (7taa) complex; **TDZ1**, **TDZ3**, **TDZ4**, **TDZ5**, **TDZ6**, **TDZ8** and **TDZ9**

TABLE-2
BINDING ENERGIES OF TITLE
COMPOUNDS (**TDZ1**-**TDZ9**) AGAINST 1B2Y

Compound code	Glide score (kcal/mol)	MMGBSA score (kcal/mol)
TDZ1	-4.71	-34.73
TDZ2	-4.841	-33.59
TDZ3	-4.535	-37.92
TDZ4	-4.573	-32.74
TDZ5	-4.618	-37.42
TDZ6	-4.663	-36.72
TDZ7	-4.515	-37.51
TDZ8	-4.563	-32.51
TDZ9	-4.822	-30.62
Co-crystal ligand	–	-99.62

for running the MD. According to that MD simulations using a simple point charge water model ran for 100 ns. The trajectory was examined as time dependent for 100 ns to determine the amount of hydrogen bonds between complexes of α-amylase and the **TDZ2**, **TDZ3**, **TDZ7** compounds as well as the root mean square deviations (RMSD) and root mean square fluctuations (RMSF). The stability of the protein backbone when bound with a particular ligand under dynamic conditions is indicated by RMSD analysis means measure the average distance between atoms of superimposed protein. During the MD simulation, it offers information on its structural conformation. Higher protein-ligand complex stability is indicated by lower RMSD values. The total RMSD study of compounds **TDZ2**, **TDZ3** and **TDZ7** at enzyme active site showed that variations in throughout 100 ns simulations fall within the typical RMSD range (Fig. 4). It shows that compounds **TDZ2**, **TDZ3** and **TDZ7** firmly adhered to the protein's binding pocket with 0.65, 0.8 and 1.5 nm, respectively indicating very good alignment and high precision docking results. As the RMSD values of **TDZ7** within 1.0-2.0 nm indicating good alignment with minor confirmational changes. The mobility and flexibility of every protein residue throughout the simulation are represented by the RMSF values. In MD simulations, a higher RMSF value denotes greater system flexibility, while a lower one implies less [33]. According to the RMSF data, the three ligand complexes are stable as fluctuations are less than 0.5 Å that means ligand jump from the active site, over the course of 100 ns (Fig. 5).

***In vitro* antidiabetic activity:** Thiadiazole derivatives (**TDZ1-TDZ9**) with different functional groups were studied for their *in vitro* α-amylase inhibition activity. All the TDZ derivatives exert moderate dose dependent inhibitory response when compared to the standard drug miglitol presented in Table-3. It is evident that maximum enzyme inhibition displayed by **TDZ7** (61%) followed by **TDZ2** (59%) and **TDZ8** (55%) at 1000 μg/mL. And the absorbance values increase with increase in concentration from 250 to 1000 μg/mL indicated by the increase in colour intensity of test solutions, which means as the concentration of **TDZ** increases, starch present in the test solution do not reduce to maltose even in presence of α-amylase enzyme which indicates the shutting down of enzyme activity represented with percentage of inhibition values (Table-3). The percentage inhibition values of standard drug, miglitol at 250, 500 and 1000 μg/mL concentration is 78, 81 and 82%, respectively.

***In vitro* antioxidant activity:** All the TDZ derivatives exert good dose dependent scavenging activity ranges from 33-68% (100 μg/mL) and 51-72% (300 μg/mL) when compared to the standard drug ascorbic acid at 300 and 100 μg/mL concentration is 78 and 76%, respectively (Table-4). It is also evident that maximum enzyme inhibition displayed by **TDZ1**

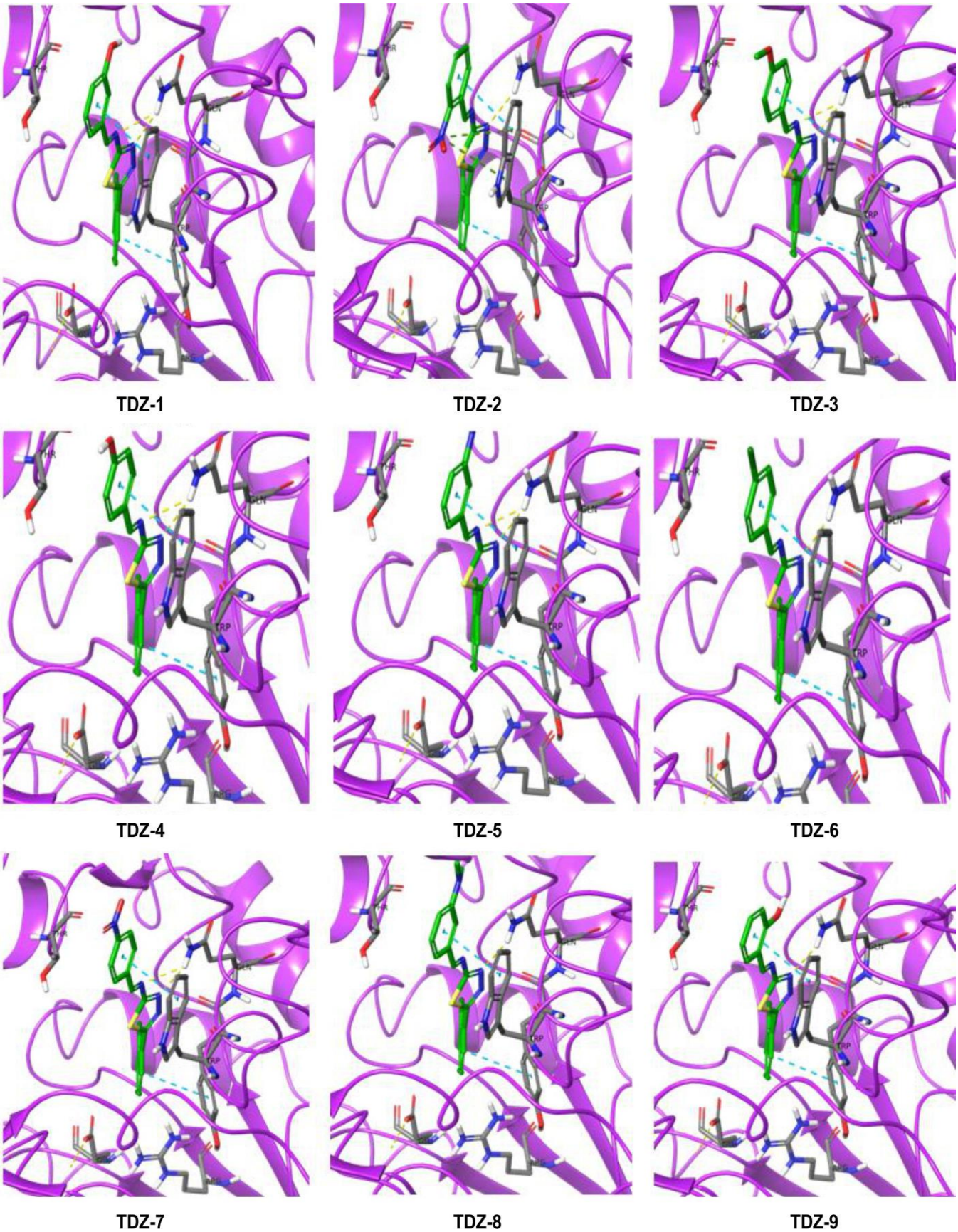

Fig. 3. Atomic interactions of title compounds with 1B2Y at the binding site; blue colour dotted lines = pi-pi interactions; yellow colour dotted lines = hydrogen bonds; green colour dotted lines = pi-lone pair interactions

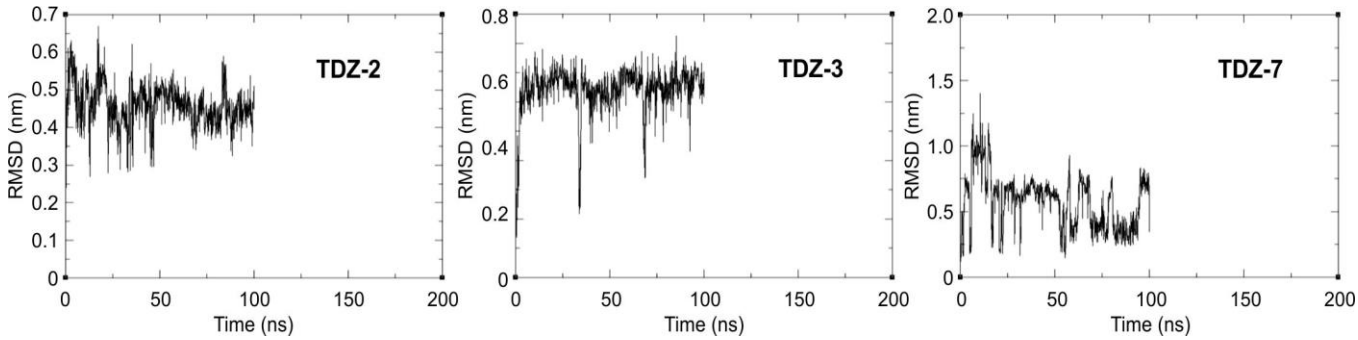

Fig. 4. Root mean square deviation (RMSD) graphs of **TDZ2**, **TDZ3** and **TDZ7** ligand protein complex at the binding site of 1B2Y

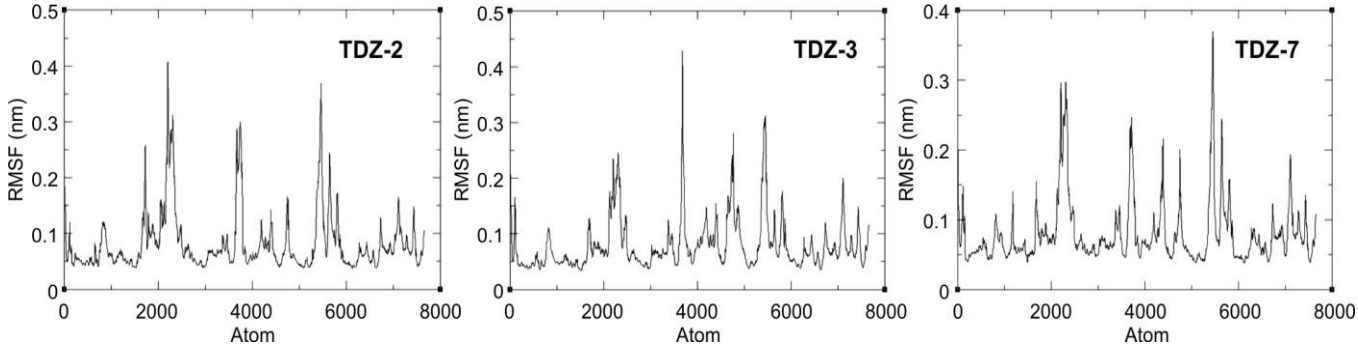

Fig. 5. Root mean square fluctuation (RMSF) graphs of **TDZ2**, **TDZ3** and **TDZ7** ligand protein complex backbone at the binding site of 1B2Y

TABLE-3
PERCENTAGE INHIBITION OF TITLE COMPOUNDS AT DIFFERENT CONCENTRATIONS IN α-AMYLASE INHIBITION ASSAY

Code	Substituent (R)	Absorbance at concentrations (μg/mL)			Percentage of inhibition at different concentrations		
		250	500	1000	250	500	1000
TDZ1	3-Hydroxy	0.354	0.349	0.325	47%	48%	52%
TDZ2	2-Nitro	0.434	0.401	0.278	36%	41%	59%
TDZ3	4-Methoxy	0.488	0.399	0.359	33%	48%	53%
TDZ4	4-Hydroxy	0.530	0.483	0.470	22%	29%	30%
TDZ5	3-Nitro	0.473	0.382	0.342	30%	43%	49%
TDZ6	4-Chloro	0.440	0.332	0.304	35%	51%	55%
TDZ7	4-Nitro	0.465	0.348	0.261	31%	49%	61%
TDZ8	8-Dimethyl amino	0.420	0.386	0.307	38%	43%	55%
TDZ9	2-Hydroxy	0.409	0.390	0.338	39%	42%	50%
Miglitol		0.145	0.130	0.124	78%	81%	82%
DMSO			0.676			–	

TABLE-4
ANTIOXIDANT ACTIVITY OF THE TITLED COMPOUNDS **TDZ1-TDZ9** BY H_2O_2 RADICAL SCAVENGING ASSAY

Code	Absorbance at concentrations (μg/mL)		Scavenging (%) at different concentrations	
	100	300	100 (μg/mL)	300 (μg/mL)
TDZ1	0.197	0.179	68	72
TDZ2	0.419	0.308	33	51
TDZ3	0.230	0.194	64	69
TDZ4	0.241	0.218	62	65
TDZ5	0.229	0.209	64	67
TDZ6	0.236	0.219	63	65
TDZ7	0.287	0.233	55	63
TDZ8	0.289	0.282	54	55
TDZ9	0.336	0.221	47	65
Ascorbic acid	0.149	0.140	76	78
DMSO	0.631		–	

(72%) followed by **TDZ3** (69%) and **TDZ5** (67%) at 300 μg/mL. Moreover, the absorbance values increased with increasing concentration from 100 to 300 μg/mL, indicating enhanced H_2O_2 scavenging activity. This trend reflects a concentration-dependent increase in the reducing power of the sample solutions.

Conclusion

Novel 1,3,4-thiadiazole derivatives (**TDZ1-TDZ9**) were synthesised and characterized successfully by IR, NMR and mass spectrometric techniques. Anti-diabetic activity of the title compounds was tested on α-amylase enzyme using miglitol as standard. Compounds **TDZ7** and **TDZ2** had shown significant activity. Molecular docking studies were conducted for α-amylase enzyme (7taa, 1b2y) and all compounds displayed least binding energy than miglitol. From the docking results, it is concluded that the hydrophobic interactions play a crucial

role in enzyme activity as miglitol forms only hydrophilic interactions and scores more binding energy than the metformin as it forms both hydrophobic and hydrophilic bonds displayed least binding energy. A comparison of the top two ligands indicates that the observed difference in binding energy arises from the number and nature of intermolecular interactions. Compound **TDZ2** forms additional hydrophobic interactions, including pi-sigma and pi-sulphur contacts, which contribute to its higher binding affinity compared to **TDZ7** and the other derivatives. Furthermore, molecular dynamics simulations confirmed that the TDZ derivatives form stable protein-ligand complexes within the active site of α-amylase, supporting the reliability of the docking results. The nitro-substituted 1,3,4-thiadiazole derivatives, particularly at the *para* (**TDZ7**) and *ortho* (**TDZ2**) positions, demonstrated superior antidiabetic activity compared to *meta*-substituted and other functionalized analogues. The enhanced activity of **TDZ2** and **TDZ7** is strongly supported by molecular docking, molecular dynamics simulations and *in vitro* α-amylase inhibition studies, indicating stable enzyme-ligand interactions and effective α-amylase inhibition. Further *in vivo* evaluation and cytotoxicity studies are required to confirm their therapeutic potential and safety.

ACKNOWLEDGEMENTS

The authors are thankful to the DST-FIST funded laboratory, Pharmaceutical Sciences Department, Acharya Nagarjuna University, Guntur for performing the synthetic work. The financial assistance for this work was provided by Seed Money Grant [No. ANU/CIIPR/Project Proposals/ Sanction of Finance Assistance/2023 Dated 26.05.2023].

CONFLICT OF INTEREST

The authors declare that there is no conflict of interests regarding the publication of this article.

DECLARATION OF AI-ASSISTED TECHNOLOGIES

The authors declare that no AI tools were used in the preparation or writing of this research/review article.

REFERENCES

1. M.D. Glossman, *J. Mol. Struct. THEOCHEM*, **330**, 385 (1995); https://doi.org/10.1016/0166-1280(94)03865-I
2. Y. Hu, C.Y. Li, X.M. Wang, Y.H. Yang and H.L. Zhu, *Chem. Rev.*, **114**, 5572 (2014); https://doi.org/10.1021/cr400131u
3. N. Kerru, L. Gummidi, S.V. Bhaskaruni, S.N. Maddila, P. Singh and S.B. Jonnalagadda, *Sci. Rep.*, **9**, 19280 (2019); https://doi.org/10.1038/s41598-019-55793-5
4. A.K. Pandey, P.P. Kashyap, C.D. Kaur, H.A. Sawarkar, H.J. Dhongade and M.K. Singh, *Int. J. Pharma. Res. Allied Sci.*, **5**, 37 (2016).
5. E.C. Pham, T.N. Truong, N.H. Dong, D.D. Vo and T.T. Hong Do, *Med. Chem.*, **18**, 558 (2022); https://doi.org/10.2174/1573406417666210803170637
6. S.M. Rana, M. Islam, H. Saeed, H. Rafique, M. Majid, M.T. Aqeel, F. Imtiaz and Z. Ashraf, *Pharmaceuticals*, **16**, 1045 (2023); https://doi.org/10.3390/ph16071045
7. T. Anthwal, S. Paliwal and S. Nain, *Chemistry*, **4**, 1654 (2022); https://doi.org/10.3390/chemistry4040107
8. A.K. Pandey, P.P. Kashyap, C.D. Kaur, H.A. Sawarkar, H.J. Dhongade and M.K. Singh, *J. Sci.*, **45**, 917 (2018).
9. Z. Ali, W. Rehman, L. Rasheed, A.Y. Alzahrani, N. Ali, R. Hussain, A.H. Emwas, M. Jaremko and M.H. Abdellattif, *ACS Omega*, **9**, 7480 (2024); https://doi.org/10.1021/acsomega.3c05854
10. U. Galicia-Garcia, A. Benito-Vicente, S. Jebari, A. Larrea-Sebal, H. Siddiqi, K.B. Uribe, H. Ostolaza and C. Martín, *Int. J. Mol. Sci.*, **21**, 6275 (2020); https://doi.org/10.3390/ijms21176275
11. F.O. Ohiagu, P.C. Chikezie and C.M. Chikezie, *Biomed. Res. Ther.*, **8**, 4243 (2021); https://doi.org/10.15419/bmrat.v8i3.663
12. S. Dhital, F.J. Warren, P.J. Butterworth, P.R. Ellis and M.J. Gidley, *Crit. Rev. Food Sci. Nutr.*, **57**, 875 (2017); https://doi.org/10.1080/10408398.2014.922043
13. R. Bashary, M. Vyas, S.K. Nayak, A. Suttee, S. Verma, R. Narang and G.L. Khatik, *Curr. Diabetes Rev.*, **16**, 117 (2020); https://doi.org/10.2174/1573399815666190618093315
14. P.M. Jayalakshmi, T.S. Jasmin and M. Jose, *Res. Pharm. Technol.*, **14**, 5293 (2021); https://doi.org/10.52711/0974-360X.2021.00923
15. S. Forli, R. Huey, M.E. Pique, M.F. Sanner, D.S. Goodsell and A.J. Olson, *Nat. Protoc.*, **11**, 905 (2016); https://doi.org/10.1038/nprot.2016.051
16. Y.H. Zaki, A.O. Abdelhamid, A.R. Sayed and H.S. Mohamed, *Polycycl. Aromat. Compd.*, **43**, 1364 (2023); https://doi.org/10.1080/10406638.2022.2027791
17. A.M. Brzozowski and G.J. Davies, *Biochemistry*, **36**, 10837 (1997); https://doi.org/10.1021/bi970539i
18. M. Duhan, P. Kumar, J. Sindhu, R. Singh, M. Devi, A. Kumar, R. Kumar and S. Lal, *Comput. Biol. Med.*, **138**, 104876 (2021); https://doi.org/10.1016/j.compbiomed.2021.104876
19. V. Nahoum, G. Roux, V. Anton, P. Rougé, A. Puigserver, H. Bischoff, B. Henrissat and F. Payan, *Biochem. J.*, **346**, 201 (2000); https://doi.org/10.1042/bj3460201
20. T.M. Archana, K.R. Haridas, T.K. Shahin Muhammed, K.R. Raghi and S. Sudheesh, *S. Afr. J. Bot.*, **164**, 386 (2024); https://doi.org/10.1016/j.sajb.2023.12.006
21. T.I. Adelusi, O.Q. Bolaji, T.O. Ojo, I.P. Adegun and S. Adebodun, *ChemistrySelect.*, **8**, e202303686 (2023); https://doi.org/10.1002/slct.202303686
22. M.B. Maraf, B.Y.G. Mountessou, T.F. Hans Merlin, P. Ariane, J.N.N. Fekoua, T.B. Jean Yves, T.T.D. Raoul, A. Abouem A Zintchem, G. Bebga, N.I. Mbouombouo and P. Ramasami, *Heliyon*, **10**, e29560 (2024); https://doi.org/10.1016/j.heliyon.2024.e29560
23. A. Rácz, L.M. Mihalovits, D. Bajusz, K. Héberger and R.A. Miranda-Quintana, *J. Chem. Inf. Model.*, **62**, 3415 (2022); https://doi.org/10.1021/acs.jcim.2c00433
24. Z. Batool, S. Ullah, A. Khan, S.N. Mali, S.S. Gurav, R.D. Jawarkar, A. Alshammari, N.A. Albekairi, A. Al-Harrasi and Z. Shafiq, *Sci. Rep.*, **14**, 25754 (2024); https://doi.org/10.1038/s41598-024-75100-1
25. R. Hussain, W. Rehman, F. Rahim, S. Khan, M. Taha, Y. Khan, A. Sardar, I. Khan and S.A. Shah, *J. Mol. Struct.*, **1293**, 136185 (2023); https://doi.org/10.1016/j.molstruc.2023.136185
26. H. Mechchate, I. Es-safi, A. Louba, A.S. Alqahtani, F.A. Nasr, O.M. Noman, M. Farooq, M.S. Alharbi, A. Alqahtani, A. Bari, H. Bekkari and D. Bousta, *Molecules*, **26**, 293 (2021); https://doi.org/10.3390/molecules26020293
27. A.S. Alqahtani, S. Hidayathulla, M.T. Rehman, A.A. ElGamal, S. Al-Massarani, V. Razmovski-Naumovski, M.S. Alqahtani, R.A. El Dib and M.F. AlAjmi, *Biomolecules*, **10**, 61 (2019); https://doi.org/10.3390/biom10010061
28. J. Hsiu, E.H. Fischer and E.A. Stein, *Biochemistry*, **3**, 61 (1964); https://doi.org/10.1021/bi00889a011
29. A. Chaudhary, A. Tiwari, K. Dobhal and V. Joshi, *Int. J. Adv. Chem. Res.*, **7**, 65 (2025); https://doi.org/10.33545/26646781.2025.v7.i5a.280
30. D.R.S. Reddy and K.H. Kumar, *Int. J. Pharm. Clin. Res.*, **6**, 71 (2014).
31. D.R. Sankara and D. Sudhakar, *Der Pharma Chem.*, **6**, 111 (2014).
32. M. Breznik, Y. Ge, J.P. Bluck, H. Briem, D.F. Hahn, C.D. Christ, J. Mortier, D.L. Mobley and K. Meier, *ChemMedChem*, **18**, e202200425 (2023); https://doi.org/10.1002/cmdc.202200425
33. D. Osmaniye, A.E. Evren, Ş. Karaca, Y. Özkay and Z.A. Kaplancıklı, *J. Mol. Struct.*, **1272**, 134171 (2023); https://doi.org/10.1016/j.molstruc.2022.134171